Supplemental Materials

OATP1B2-deficiency protects against paclitaxel-induced neurotoxicity

Alix F. Leblanc,[1] Jason A. Sprowl,[2] Paola Alberti,[3] Alessia Chiorazzi,[3] W. David Arnold,[4] Alice A. Gibson,[1] Kristen W. Hong,[1] Marissa S. Pioso,[1] Mingqing Chen,[1] Kevin M. Huang,[1] Vamsi Chodisetty,[1] Olivia Costa,[2] Tatiana Florea,[2] Peter de Bruijn,[5] Ron H. Mathijssen,[5] Raquel E. Reinbolt,[6] Maryam B. Lustberg,[6] Lara E. Sucheston-Campbell,[7] Guido Cavaletti,[3] Alex Sparreboom,[1] and Shuiying Hu[1]

[1]Division of Pharmaceutics and Pharmaceutical Chemistry, College of Pharmacy and Comprehensive Cancer Center, the Ohio State University, Columbus, OH; [2]Department of Pharmaceutical, Social and Administrative Sciences, School of Pharmacy, D'Youville College, Buffalo, NY; [3]Experimental Neurology Unit and Milan Center for Neuroscience, School of Medicine and Surgery, University of Milano-Bicocca, Monza, Italy; [4]Division of Neuromuscular Disorders, Department of Neurology, College of Medicine, the Ohio State University, Columbus, OH; [5]Department of Medical Oncology, Erasmus MC Cancer Institute, Rotterdam, The Netherlands; [6]Department of Internal Medicine, College of Medicine, the Ohio State University, Columbus, OH; [7]Division of Pharmacy Practice and Science, College of Pharmacy, the Ohio State University, Columbus, OH.

Supplemental Figure 1

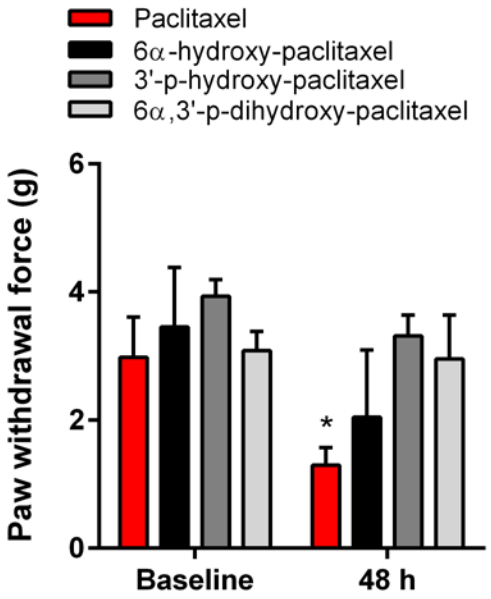

Influence of paclitaxel metabolites on treatment-related neurotoxicity. Mechanical allodynia was evaluated after a single dose of paclitaxel or its metabolites 6α-hydroxy-paclitaxel, 3'-p-hydroxy-paclitaxel, and 6α,3'-p-dihydroxy-paclitaxel (all administered at a dose of 10 mg/kg, i.v.). All data represent mean values (bars) and SD, using n=5 per group. The star (*) denotes significant differences from baseline ($P<0.05$) as evaluated with an unpaired two sided Student's *t*-test with Welch's correction.

Supplemental Figure 2

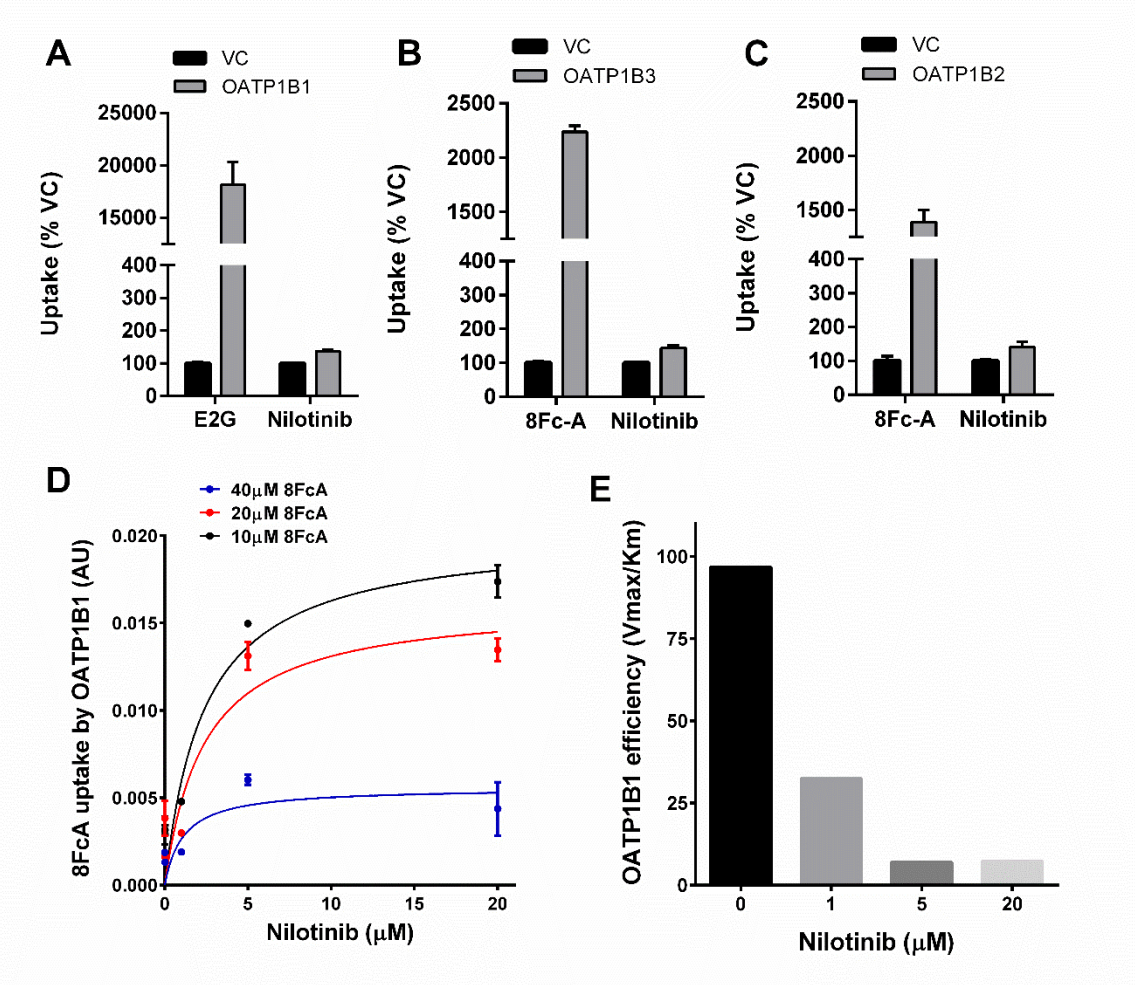

Interaction of nilotinib with OATP1B-type transporters. Cellular uptake of the prototypical substrates estradiol-17β-D-glucuronide (E2G; 0.1 µM; 15 min uptake) or 8-(2-[fluoresceinyl]-aminoethylthio)-adenosine-3',5'-cyclic monophosphate (8Fc-A; 25 µM; 30 min uptake) or the TKI nilotinib (0.1 µM; 30-min uptake) was evaluated in HEK293 cells transfected with OATP1B1 (**A**), OATP1B3 (**B**), or OATP1B2 (**C**). The concentration-dependence of nilotinib-based on inhibition of OATP1B1 function in arbitrary units (AU) was evaluated in the same models using varying concentrations of 8Fc-A (**D**). The observed data were transformed to derive nilotinib-dependent values for OATP1B1 function by calculating the ratio of the maximal velocity of transport (Vmax) by the Michaelis-Menten constant Km (**E**). Data (n=4-12 per group) were normalized to substrate uptake in cells transfected with an empty vector (VC), which was set at 100%. All data represent mean values (bars or symbols) and SD (error bars).

Supplemental Figure 3

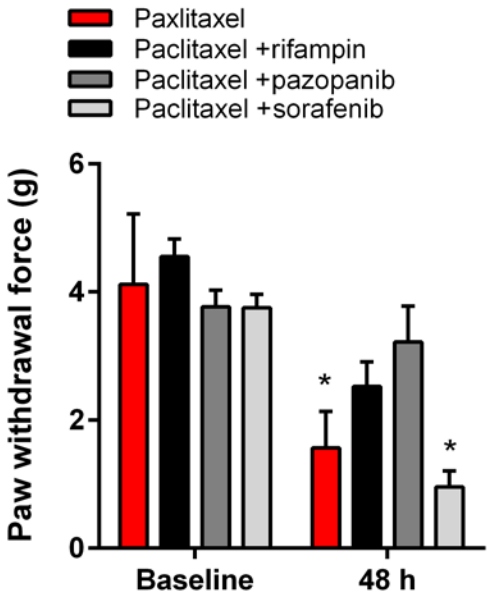

Influence of OATP1B-type inhibitors on paclitaxel-related neurotoxicity. Mechanical allodynia was evaluated after a single dose of paclitaxel (10 mg/kg, i.v.) preceded by rifampin (20 mg/kg; i.p.), pazopanib (20 mg/kg; p.o.) or sorafenib (20 mg/kg; p.o.), all given 30-min before paclitaxel. All data represent mean values (bars) and SD, using n=5 per group. The star (*) denotes significant differences from the respective baseline ($P<0.05$) as evaluated with an unpaired two sided Student's *t*-test with Welch's correction.

Supplemental Figure 4

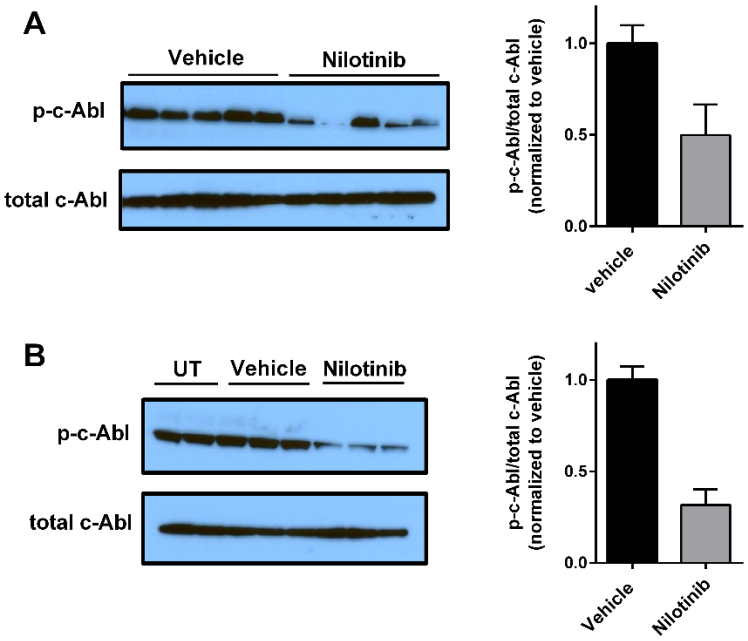

Influence of nilotinib administration on phosphorylation of c-Abl in liver and DRG of mice. Protein levels were evaluated in liver (A) and DRG (B) in untreated (UT), vehicle treated, or nilotinib treated (100 mg/kg; p.o.) wild-type mice, using specific antibodies for phospho-c-Abl (p-c-Abl) and total c-Abl. The bar graphs represent quantifications as mean values (bars) and SD, using all observations per group (n=2-5).

Supplemental Figure 5

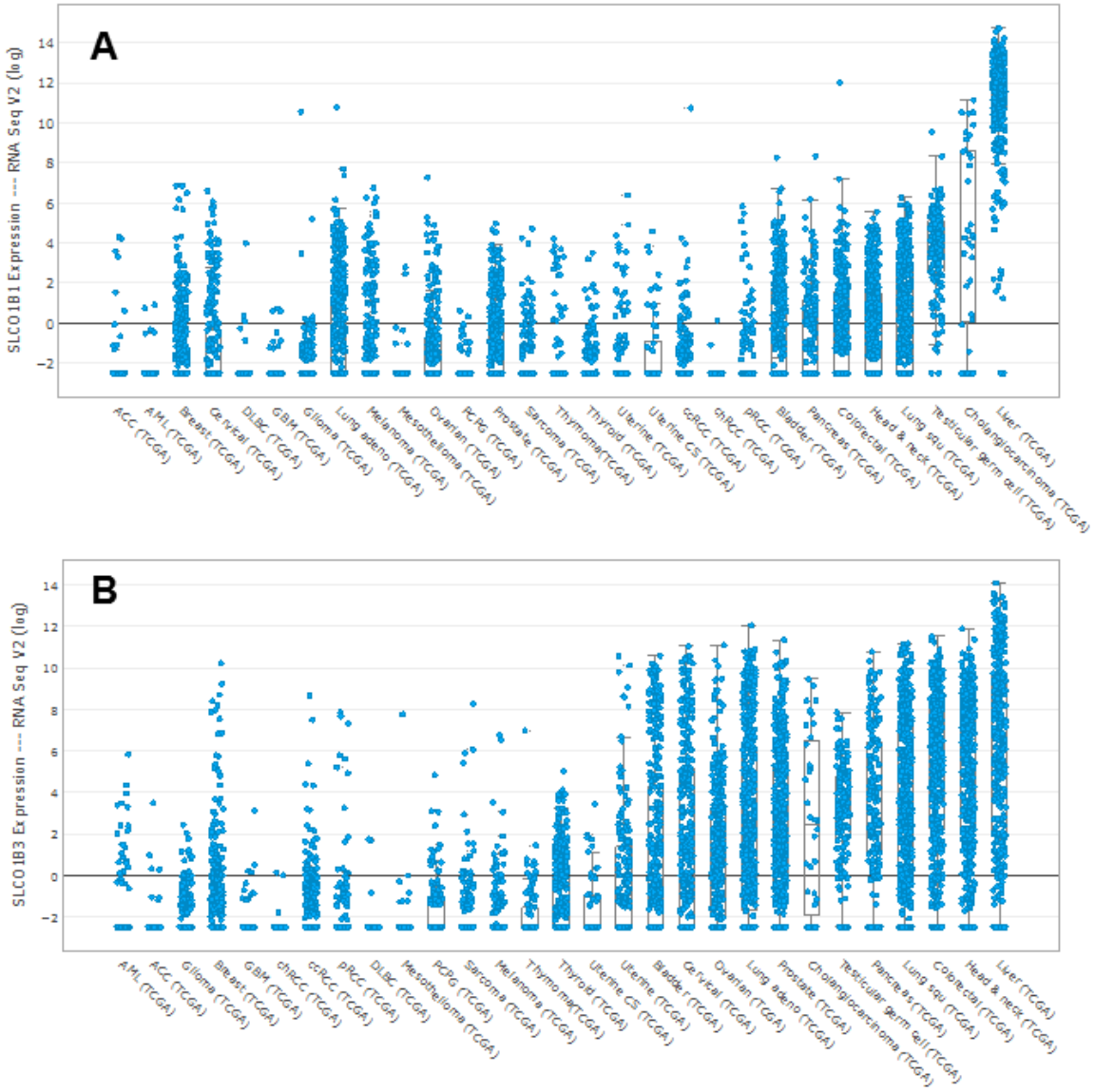

Expression of the OATP1B1 and OATP1B3 genes in human cancers. Data for the OATP1B1 (*SLCO1B1*) (**A**) and OATP1B3 (*SLCO1B3*) (**B**) genes were obtained from human tumor specimens using normalized RNAseq data from 29 individual pan-cancer (PanCan) cohorts from The Cancer Genome Atlas (TCGA). The expression values were normalized across cancer types, and ordered by their median expression from left to right (log scale). Each tumor is represented by an individual blue dot.

Supplemental Figure 6

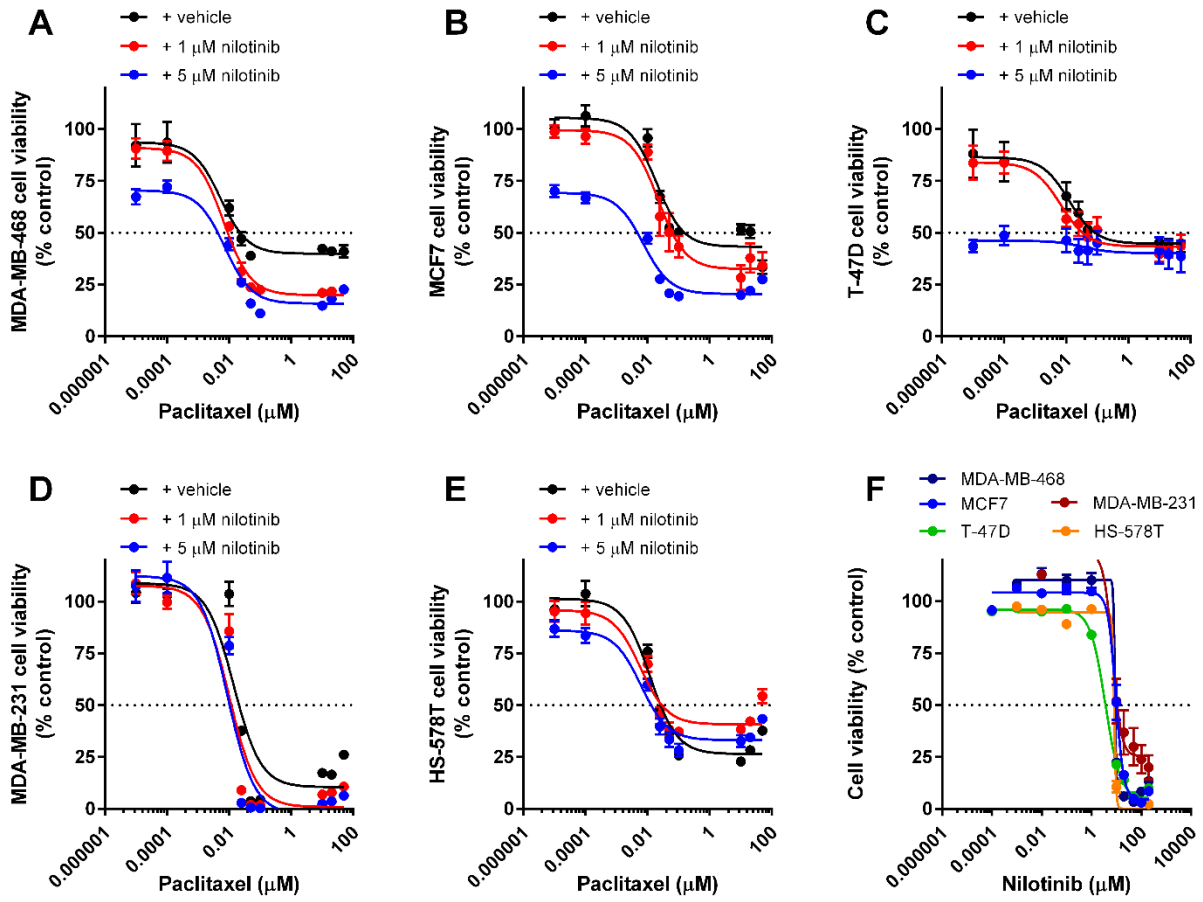

Cytotoxicity of nilotinib-paclitaxel in breast cancer models. Influence of nilotinib (1 or 5 μM; 15-min pre-incubation) on the cytotoxicity of paclitaxel in the replicating breast cancer cell lines MDA-MB-468 (**A**), MCF7 (**B**), T-47D (**C**), MDA-MB-231 (**D**), and HS-578T (**E**), and cytotoxicity of nilotinib alone in the same cell lines (**F**). Data (n=6-12 per group) represent mean (bars) and SEM (error bars) from an MTT assay following 72-h continuous exposure.

Supplemental Figure 7

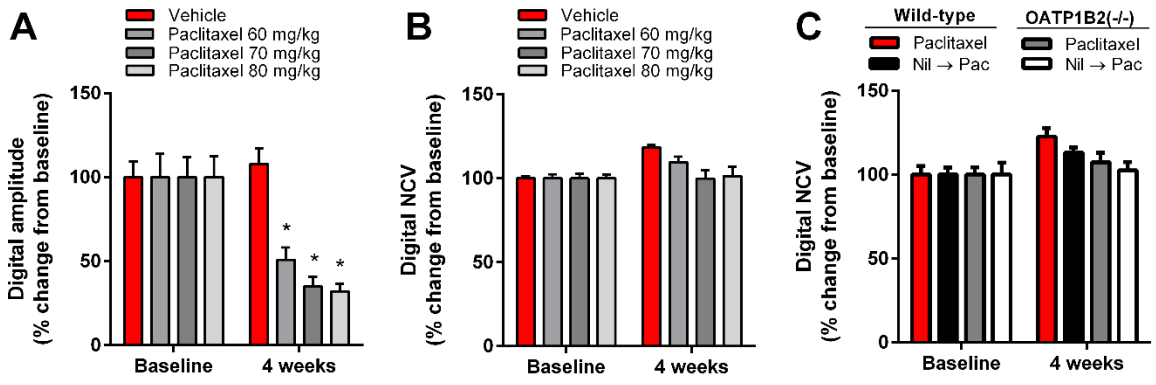

Dose-dependence of paclitaxel-induced neurotoxicity phenotypes. Changes in digital nerve maximal action potential amplitudes (**A**) and digital nerve conductance velocity (NCV) (**B**) were recorded in wild-type mice after 4 weekly i.v. paclitaxel doses of 60, 70, or 80 mg/kg. Subsequent analyses confirmed that digital NCV is not affected by paclitaxel (Pac; 70 mg/kg; i.v. once weekly) in the presence or absence of pre-treatment with nilotinib (Nil; 100 mg/kg; p.o.) in wild-type or OATP1B2(-/-) mice (**C**). All data represent mean values (bars) and SD (error bars), using n=6-16 per group. The star (*) denotes significant differences from baseline and vehicle ($P<0.05$) as evaluated with an unpaired two sided Student's *t*-test with Welch's correction.

Supplemental Figure 8

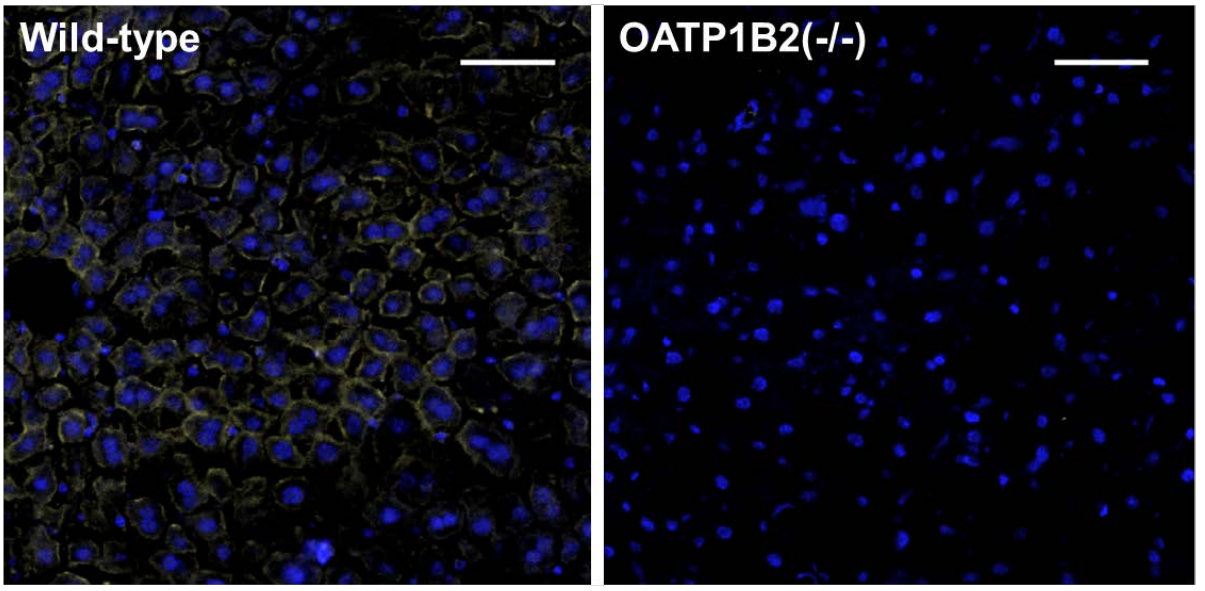

Phenotypic characterization of OATP1B2(-/-) mouse liver. Detection of OATP1B2 by immunofluorescence in liver of wild-type and OATP1B2(-/-) mice. OATP1B2 is depicted by yellow fluorescence, whereas DNA is depicted in blue (DAPI). The scale bar represents 50 µm.

Supplementary Table 1. Genes included on the Mouse Transporter RT^2 Profiles PCR array system.

Number	Symbol	Number	Symbol	Number	Symbol	Number	Symbol	Number	Symbol
1	*Abca1*	21	*Abcc12*	41	*Slc5a1*	61	*Slc22a3*	81	*Slco3a1*
2	*Abca2*	22	*Abcd1*	42	*Slc5a4a*	62	*Slc22a6*	82	*Slco4a1*
3	*Abca3*	23	*Abcd3*	43	*Slc7a11*	63	*Slc22a7*	83	*Slco22a4*
4	*Abca4*	24	*Abcd4*	44	*Slc7a4*	64	*Slc22a8*	84	*Slco29a3*
5	*Abca9*	25	*Abcf1*	45	*Slc7a5*	65	*Slc22a9*	85	*Tap1*
6	*Abca12*	26	*Abcg2*	46	*Slc7a6*	66	*Slc25a13*	86	*Tap2*
7	*Abca13*	27	*Abcg8*	47	*Slc7a7*	67	*Slc28a1*	87	*Vdac1*
8	*Abcb1a*	28	*Aqp1*	48	*Slc7a8*	68	*Slc28a2*	88	*Vdac2*
9	*Abcb1b*	29	*Aqp7*	49	*Slc7a9*	69	*Slc29a1*	89	*Gusb**
10	*Abcb4*	30	*Aqp9*	50	*Slc10a1*	70	*Slc29a2*	90	*Hprt1**
11	*Abcb5*	31	*Atp6v0c*	51	*Slc10a2*	71	*Slc31a1*	91	*Hsp90ab1**
12	*Abcb6*	32	*Atp7a*	52	*Slc15a1*	72	*Slc38a2*	92	*Gapdh**
13	*Abcb11*	33	*Atp7b*	53	*Slc15a2*	73	*Slc38a5*	93	*Actb**
14	*Abcc1*	34	*Mvp*	54	*Slc16a1*	74	*Slco1a4*	94	*MGDC**
15	*Abcc2*	35	*Ralbp1*	55	*Slc16a2*	75	*Slco1a5*	95	*RTC**
16	*Abcc3*	36	*Slc2a1*	56	*Slc16a3*	76	*Slco1a6*	96	*PPC**
17	*Abcc4*	37	*Slc2a2*	57	*Slc19a1*	77	*Slco1b2*		
18	*Abcc5*	38	*Slc2a3*	58	*Slc19a2*	78	*Slco1c1*		
19	*Abcc6*	39	*Slc3a1*	59	*Slc22a1*	79	*Slco2a1*		
20	*Abcc10*	40	*Slc3a2*	60	*Slc22a2*	80	*Slco2b1*		

* Included as controls/house-keeping genes.

Supplemental Table 2. Influence of OATP1B2-deficiency on the pharmacokinetics of paclitaxel in mice.*

Parameter	Wild-type	OATP1B2(-/-)
C_{max} (µg/ml)	35.8 ± 8.59	36.9 ± 10.8
AUC (µg·h/ml)	18.8 ± 4.90	25.6± 5.23*
CL (l/h/kg)	0.565 ± 0.174	0.406 ± 0.096*
$T_{1/2}$ (h)	1.30 ± 0.365	1.39 ± 0.294

Abbreviations: C_{max}, peak plasma concentration; AUC, area under the plasma concentration-time curve; CL, clearance; $T_{1/2}$, terminal half-life.

*Parameters are presented as mean ± SD and were derived from concentrations determined in plasma obtained at various time points after administration of a single dose of paclitaxel (10 mg/kg) in DBA/LacJ (wild-type) mice or age-matched OATP1B2(-/-) mice (n=4 per group). The AUC was calculated using non-compartmental pharmacokinetic analysis extrapolated out to 2 hours. Parameter estimates were obtained using the software package WinNonlin 6.2 (Pharsight). The star (*) denotes significant differences from wild-type (P<0.05) as evaluated with an unpaired two sided Student's *t*-test with Welch's correction.

Supplemental Table 3. Influence of nilotinib on the pharmacokinetics of paclitaxel in mice.*

Parameter	Wild-type		OATP1B2(-/-)	
	+ Vehicle	+ Nilotinib	+ Vehicle	+ Nilotinib
C_{max} (µg/ml)	28.9 ± 7.27	32.0 ± 10.7	40.1 ± 15.1	44.0 ± 11.9
AUC (µg·h/ml)	16.2 ± 4.08	16.9 ± 6.43	30.0± 9.83*	28.4 ± 13.7*
CL (l/h/kg)	0.466 ± 0.084	0.527 ± 0.239	0.229 ± 0.108*	0.265 ± 0.21*
$T_{1/2}$ (h)	1.13 ± 0.253	0.985 ± 0.313	1.34 ± 0.143	1.86 ± 0.919

Abbreviations: C_{max}, peak plasma concentration; AUC, area under the plasma concentration-time curve; CL, clearance; $T_{1/2}$, terminal half-life.

*Parameters are presented as mean ± SD and were derived from concentrations determined in plasma obtained at various time points after administration of a single dose of paclitaxel (10 mg/kg) with or without pretreatment with nilotinib (100 mg/kg; p.o.) in DBA/LacJ (wild-type) mice or age-matched OATP1B2(-/-) mice (n=5 per group). The AUC was calculated using non-compartmental pharmacokinetic analysis extrapolated out to 2 hours. Parameter estimates were obtained using the software package WinNonlin 6.2 (Pharsight). The star (*) denotes significant differences from wild-type (P<0.05) as evaluated with an unpaired two sided Student's *t*-test with Welch's correction.

Supplemental Table 4. Expression of OATP1B1 and OATP1B3 in human breast cancers.*

No.	Age	Stage	ER status	PR status	HER2 status	Ct values		
						OATP1B1	OATP1B3	GAPDH
C1	42	I	Positive	Positive	Negative	ND	ND	24.195
C2	40	I	Negative	Negative	Negative	ND	37.600	24.163
C3	70	I	Negative	NA	Negative	ND	ND	24.208
C4	41	I	NA	Positive	Negative	ND	ND	23.737
C5	66	I	Positive	Positive	Negative	ND	43.956	25.372
C6	20	I	Negative	Negative	Negative	ND	ND	24.969
C7	72	I	Positive	Positive	Negative	ND	ND	25.303
C8	58	I	Negative	NA	Negative	ND	ND	23.433
C9	70	I	Negative	Negative	Negative	ND	ND	24.856
C10	56	I	Negative	NA	Positive	ND	ND	24.643
C11	74	I	Negative	Negative	Positive, strong (3+)	ND	ND	26.587
C12	45	I	Positive	Positive	Positive, weak (2+)	ND	ND	24.103
D1	33	IIA	Positive	NA	Negative	ND	ND	24.208
D2	68	IIA	Positive	NA	Negative	ND	ND	23.714
D3	74	IIA	Positive	Negative	Negative	35.712	40.789	25.539
D4	50	IIA	Positive	NA	Negative	ND	ND	24.957
D5	36	IIA	Negative	Negative	Negative	ND	ND	25.349
D6	52	IIA	Negative	Negative	Positive, strong (3+)	ND	ND	25.449
D7	61	IIB	Negative	NA	Negative	38.242	38.578	23.565
D8	80	IIB	Positive	Positive, weak	Negative	ND	ND	24.188
D9	33	IIB	Negative	Negative	Negative	ND	35.093	24.014
D10	33	IIB	Negative	Negative	Positive	ND	ND	25.769
D11	71	IIB	Positive	Positive, weak	Positive, strong (3+)	ND	ND	25.353
D12	57	IIB	Negative	Negative	Positive, strong (3+)	ND	ND	24.555
E1	57	IIB	Negative	Negative	Positive, strong (3+)	ND	ND	25.745
E2	89	IIB	Positive	Positive	Positive, weak (2+)	ND	ND	24.275

E3	49	IIB	Negative	Negative	Positive, weak (2+)	39.214	ND	24.751
E4	56	IIB	NA	NA	NA	ND	ND	23.698
E5	68	IIIA	Positive	NA	Negative	ND	39.246	24.744
E6	86	IIIA	NA	NA	Negative	ND	ND	24.407
E7	66	IIIA	Negative	Negative	Negative	37.440	ND	25.985
E8	85	IIIA	Positive	Positive	Positive, weak (2+)	ND	ND	24.957
E9	54	IIIA	Positive	Positive	Positive, weak (2+)	ND	ND	24.109
E10	60	IIIA	Positive	NA	Not reported	ND	ND	24.905
E11	50	IIIA	NA	NA	Not reported	36.652	ND	24.988
E12	66	IIIB	Negative	Negative	Positive, strong (3+)	37.884	ND	25.035
F1	56	IIIB	Negative	Borderline	Positive, strong (3+)	ND	ND	25.069
F2	86	IIIB	NA	NA	NA	ND	ND	23.549
F3	54	IIIC	Positive	Positive, focal	Negative	ND	ND	25.430
F4	81	IIIC	Positive	Positive	Negative	ND	39.938	23.537
F5	36	IIIC	Negative	Negative	Positive, weak (2+)	36.777	ND	24.965
F6	52	IIIC	NA	NA	NA	ND	38.834	24.673
F7	38	IIIC	NA	NA	NA	ND	ND	23.878
F8	62	IV	Positive	Not reported	Negative	ND	ND	24.808
F9	70	IV	Negative	Positive	Negative	37.576	39.935	26.470
F10	55	IV	NA	Not reported	Not reported	ND	ND	23.307
F11	46	IV	Not reported	Not reported	Not reported	32.876	29.523	23.469
F12	60	IV	Not reported	Not reported	Not reported	ND	ND	25.747

Abbreviations: ER, estrogen receptor; PR, progesterone receptor; NA, not available; ND, not detectable.

*Tissue plates containing cDNA from 48 human breast cancer tissues (Tissue Scan Arrays BCRT-303) were obtained from Origene. RNA was reverse transcribed, and gene transcripts were quantified with primers specific to OATP1B1 (*SLCO1B1*) and OATP1B3 (*SLCO1B3*). Reactions were carried out in triplicate, and shown relative to transcripts of the housekeeping gene, *GAPDH*.